HIGH SCHOOL EDITION
Journal of Student Research
Volume 13 Issue 4 (2024)

Mathematical Modelling Simulation of Oncolytic Virotherapy Cancer Treatment

Aryav Odhrani[1] and Khoi Vo[#]

[1]Dubai College, UAE
[#]Advisor

ABSTRACT

Oncolytic virotherapy is a cancer treatment that uses replicating viruses to target and kill tumour cells. The interaction between tumour cells and an oncolytic virus can be represented in a mathematical model. In this paper we study the development of some mathematical models and their dynamics. We study the conclusions of various approaches to the modelling, including a system of ordinary differential equations, the dynamical system's theory, and a predatory-prey model. The study analyses thresholds that enable us to identify solutions of a virus-cell interaction function. We run Hopf bifurcation to classify stable equilibrium points in the function. We also propose a mathematical model on oncolytic virotherapy incorporating multiple cell populations and free viruses. Optimal viral burst sizes to reduce tumour load in the quickest time are obtained. Burst sizes around 25 were found to be optimal, and 3 viral drugs, including a modified HSV and an adenovirus ONYX-015, were presented as the most effective treatments.

Introduction

Oncolytic virotherapy is a cancer treatment that uses replicating viruses to target and kill tumour cells. In oncolytic virotherapy, free viruses are injected into a patient, and infect tumour cells. They replicate themselves there and eventually new virion particles burst out, causing the lysis of the infected cell, and proceeding to infect other tumour cells. Oncolytic virotherapy treatment, hereinafter referred to as "OVT", has proven to have initial success in its development.

The OVT field has progressed and developed over the last couple of decades. The idea was first tested in the middle of the 20th century [1] after accidental viral infections positively benefitted cancer patients. Over time, the idea has developed as scientific knowledge and technology has improved, such that medicine now provides viral drugs targeting specific cancer cells. Certain species of virus are genetically modified and used as anti-cancer therapeutic agents based on their efficiency in destroying a cancer tumour. Various viruses have shown promising results in clinical trials over the last couple decades. Among these viruses include the herpes simplex virus HSV 1, the Newcastle disease virus NDV, the M1 virus, and, most prominently, the Onyx-15 adenovirus [2].

A tumour can spread to different parts of the body if it is malignant. There is a mere 50% chance of surviving cancer for 10 or more years [3], and this low rate can be increased by optimising cancer treatment – especially in the new field of OVT. Thus, models like ours are an important part of improving the developing treatment by identifying optimal viruses. A mathematical model in particular helps increase the efficacy of the treatment by simulating the change in tumour load over time based on initial conditions, so a mathematical model would provide doctors insights into understanding the effects of a virus on a tumour. The model's results determine which viral drugs are the most effective at eradicating a tumour. In this paper, we develop a deterministic mathematical model to simulate OVT and assess its impact on a tumour.

There are different strategies to using viruses to control a tumour. First, a common method is to have the virus infect cells, replicate, and kill the cells by lysis, leading to possible tumour elimination. The second method can occur with low-level virus reproduction in cells that results in the production of a cytotoxic protein that can kill tumour cells. Third, a viral infection in the tumour region can induce an anti-tumour immune response from the body, which could control and eradicate the tumour.

Background

Mathematical modelling in science has often been helpful in analysing the outcomes of disease and treatment in the field of theoretical epidemiology, the study of health and disease. In order to gain a complete understanding of how the virus and cells interact in OVT, extensive efforts have been made to establish several mathematical models that have given rise to optimal strategies. In this paper, we look at four studies conducted into modelling OVT.

First, in 2003, Wodarz et al. presented a simple model of differential equations to represent the relationships between cell species in the tumour region [4]. Apart from Wodarz et al., several other models have been proposed that also present the model as a system of differential equations, such as Norman et al. [5] and Wein et al. [6]. Second, we study Novozhilov et al.'s paper [7]. Their paper is a more complex, stochastic model that considers unknown situations such as random mutations and cell proliferation. Third, we look at Abu-Rqayiq's paper [1], which shows the dynamical system's theory. It studies the thresholds that assist in classifying asymptomatic dynamics, which are variables that have no visible effect on the result graphs. Fourth, we explore Friedman and Kao's study on modelling OVT, a chapter from their book, *'Mathematical Modeling of Biological Processes'* [8]. This model develops upon Wodarz's basic model; it uses differential equations but involves more cell species. Friedman also cowrote a paper with Tao, where they studied took a different approach and developed ratio-dependent predator-prey model, presenting for it a rigorous mathematical analysis [9]. These papers have helped us identify the best virus burst sizes that lead to the quickest tumour eradication; however, they use a variety of different initial parameters and conditions. We will study these variations and assess their efficacies to find the optimum combination of conditions for our model.

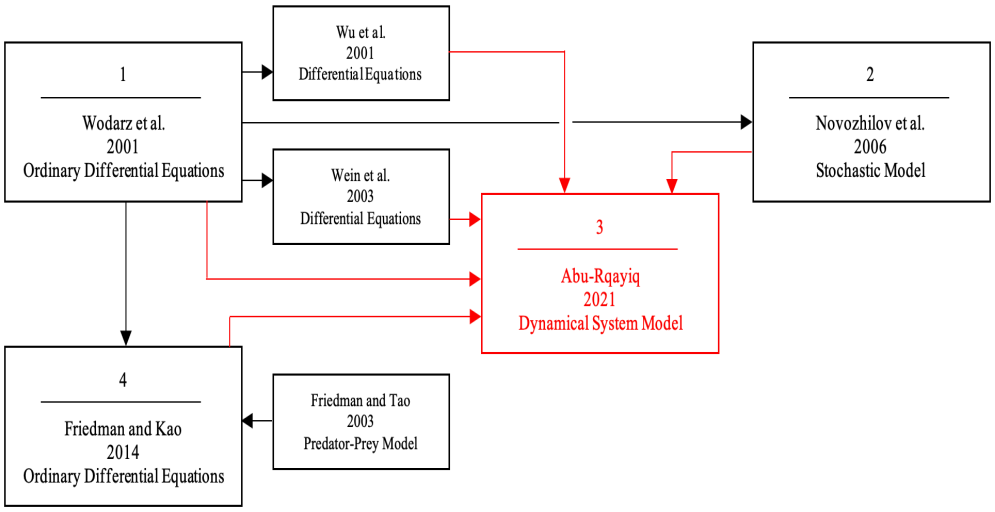

Figure 1. A summary and relations of different mathematical models and papers representing oncolytic virotherapy cancer treatment

Wodarz et al. (2003)

Wodarz et al. proposed a system modelling the dynamics of oncolytic virus replication [4]. In the system, Wodarz et al. presented multiple ordinary differential equations, hereinafter referred to as "ODEs", that described the development of virus and cell populations in a tumour over time.

Proposition 2.1.

The model took a simple approach and is generally based on the law of mass action [1] *as shown in*

$$\frac{dx}{dt} = xF(x,y) - \beta yG(x,y), \quad (1)$$

$$\frac{dy}{dt} = \beta yG(x,y) - ay. \quad (2)$$

Here the differential equation (1) represents the rate of population growth of uninfected tumour cells, and (2) represents the rate of population growth of infected tumour cells. In this system, the function *F* describes the development of uninfected tumour cells, and the function *G* describes the rate at which uninfected tumour cells become infected by the virus. The parameter β represents the infectivity of the virus, and *ay* represents the rate at which infected tumour cells die. Wodarz et al. also included the free virus population *v* in their model. This basic model states that the growth of uninfected tumour cells is the development of the cell species subtracted by the rate at which they change to another species by becoming infected. Similarly, the growth of infected tumour cells is calculated by the rate at which uninfected cells become infected subtracted by the rate at which they die. The model is based upon the law of mass action, which states that the rate of a reaction – in this case the growth of each species – is proportional to the product of the concentration of each species. This means that $\frac{dx}{dt}$ is proportional to the increase in uninfected tumour cells x (by a factor of the rate *F*) and the decrease in x (by a factor of β and the rate *G*). Similarly, the change in the second species $\frac{dy}{dt}$ is proportional to the increase in infected tumour cells y (by a factor of β and the rate *G*) and the decrease in y (by a factor of a).

Wodarz et al.'s paper studied the conditions leading to tumour remission. The paper concluded that optimal conditions depend on whether a virus replicates or not, viz., the burst size of the virus. If the virus does not replicate at all, then the rate of killing tumour cells with the virus should be maximised. Here, each virus particle would enter and kill a single tumour cell before proceeding to the next. If the virus does replicate, then the rate of killing tumour cells the virus should be kept small, as the virus would grow by itself. In the case that the virus is too lytic in tumour cells, then the persistence of both the virus and tumour are a certainty.

Novozhilov et al. (2006)

The paper *'Mathematical modeling of tumor therapy with oncolytic viruses: Regimes with complete tumor elimination within the framework of deterministic models'* [7] presents a complete parametric analysis of the dynamic variables in the society of interacting cells, explaining the effects of different parameters on the growth of a tumour over time. This model is unique as the results exhibit all three possible outcomes of OVT: no effect on the tumour, stabilisation, or reduction of the tumour size, and most desirably, a complete elimination of tumour.

Novozhilov et al.'s paper approaches the modelling differently from most ODE systems; they consider both random mutations and cell proliferation in a stochastic model. Stochastic models have been useful in more

realistically simulating cancer tumour progression but are more complicated to develop. This is because stochastic models must consider the effects of random variances and anomalies in several parameters at each timestep, increasing the number of different outcomes greatly, and leading to the addition of more mathematics to simulate the changes accurately. Novozhilov et al.'s model addresses the interaction between viruses and tumour cells as complex and non-linear process.

The studies Novozhilov et al. conducted resulted in the finding of six different domains (situations) that show the possible regions of parameter values which produce different system equilibria in their model, shown in Figure 2 [7]. System equilibria represent the roots of the derivative functions, such as $\frac{dx}{dt}$. The domains (graphs) show the progression of the roots towards a stable equilibrium as parameters change. Domains I and II represent a situation where the infection is asymptomatic, and the region is absent of infected cells. Domain III presents a system where either all cells - or none - are infected. Domain IV shows where the final state of all cells is infected, and Domains V and VI present the situation of a globally stable equilibrium and the coexistence of both populations. A point is stable if nearby solutions all converge towards it, and unstable if they are diverging. A stable equilibrium means that the situation will hold, and there is little chance in population of species. The analysis of these graphs helps find stable points, and thus graph the function of the growth of the tumour over time based on the initialisation of different parameters.

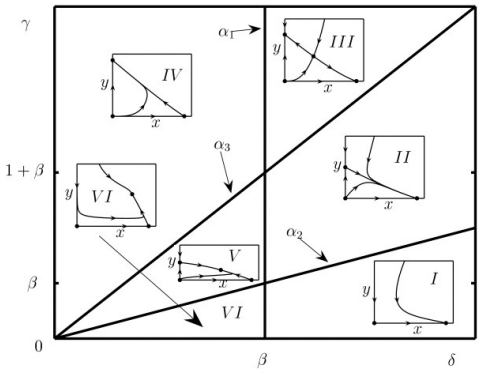

Figure 2. A graph showing the different domains which produce different system equilibria, created by Novozhilov, 2006

Novozhilov et al. display their results in the graphs in Figure 3 [7]. The partially successful eradication of the tumour, shown in graph (a), which began with an increase in tumour load, was achieved with initial conditions $\gamma = 0.7$, $\beta = 15$, $\delta = 10$, and the successful OVT outcome leading to an immediate decrease in tumour size, shown in graph (b), was achieved with initial conditions $\gamma = 0.7$, $\beta = 1005$, $\delta = 1000$, where γ is the growth rate of infected cells, β is the transmission rate of the virus and δ is the rate of infected cell killing, all compared to the growth of uninfected cells (also the tumour). The model's initial conditions are set to $x(0) = 0.1$ and $y(0) = 0.0001$. The values of parameters and initial conditions are important to our paper, as we attempt to use them in our model and explain their effects through our graphs.

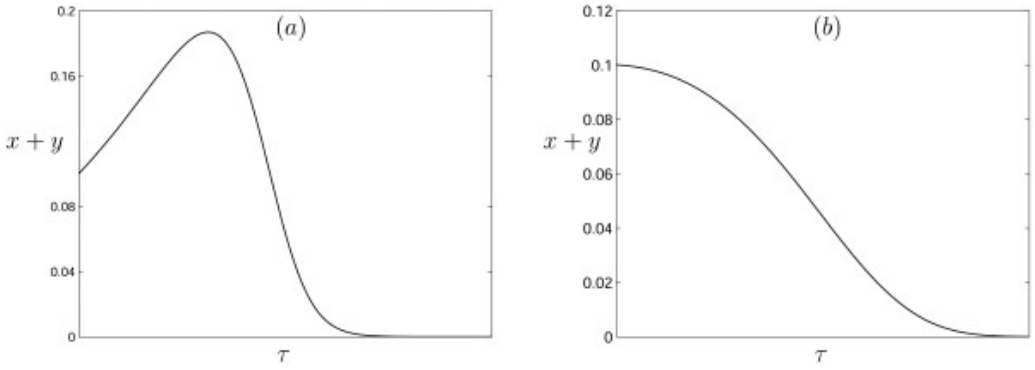

Figure 3. A graph showing the results of Novozhilov's model simulation, created by Novozhilov, 2006

Abu-Rqayiq (2021)

Abu-Rqayiq studied several models to represent OVT in *'Mathematical Modeling and Dynamics of Oncolytic Virotherapy'* [1]. He explains a basic model that is attributed to Tian, which incorporates burst size. The burst size of a virus is the number of new viruses released from the lysis of an infected cell. Burst sizes vary between different species of viruses but are very similar in the same species.

Proposition 2.2.

Tian's model [12] *is non-dimensionalised for simplicity and shown as*

$$\frac{dx}{dt} = rx(1 - x - y) - axv, \quad (3)$$

$$\frac{dy}{dt} = axv - y, \quad (4)$$

$$\frac{dv}{dt} = by - axv - cv, \quad (5)$$

where the differential equation (5) represents the rate of population growth of free viruses. Here r (also λ) is the tumour growth rate and c (also γ) is the clearance rate of the virus. This model can be represented in a Jacobian matrix, which collects all partial derivatives of the vector function of tumour growth. Abu-Rqayiq studies the equations to find parameter values leading to stable points in the function, which indicate partial or complete success of OVT. The parameters used in this model are described in Figure 4 [1], and successfully provide periodic solutions for the function as a result of Hopf bifurcation, where periodic solutions appear as a parameter passes a critical value.

Parameter	Description	Value	Dimentions
λ	Tumor growth rate	2×10^{-2}	$1/h$
δ	Death rate of infected tumor cells	1/18	$1/h$
β	Infection rate of the virus	$7/10 \times 10^{-9}$	$mm^3\ h/$ virusl
k	Immune killing rate of virus	10^{-8}	$mm^3\ h/$ immune cell
b	Burst size of free virus	50	viruses/cell
γ	Clearance rate of virus	2.5×10^{-2}	$1/h$

Figure 4. An image showing Abu-Rqayiq's model parameters, created by Abu-Rqayiq, 2021

Abu-Rqayiq also studies a model accounting for the innate immune response, which has a negative effect on OVT by killing infected tumour cells, hindering the treatment by preventing the virus from spreading in the tumour. The analysis shows that below a certain burst size threshold, the tumour always grows to its maximum size, and above the threshold, solutions lead to an undetectable tumour size. The model successfully produces a locally stable equilibrium (where the function tends towards a single point), which is critical and useful in evaluating the function of tumour growth over time. Abu-Rqayiq also studies the solutions of a fractional-derivative approach, and optimisation by control theory, both of which independently analyse ways to minimise a tumour and the cost of OVT. The paper determines that with parameters r = 0.36, a = 0.1, c = 0.2 and burst size b = 9, the basic model gives stable equilibrium points between thresholds $5 < b < 27.766$. In our model, we use several burst sizes between these thresholds and analyse the results, and whether the tumour load reduces.

Friedman and Kao (2014)

Friedman and Kao presented a system of ODEs in their 2014 book *'Mathematical Modeling of Biological Processes'* [8]. They considered a very simple model with four cell species represented by variables: x = cancer cells, y = infected cancer cells, n = dead cells, v = free viruses, $z(r,t)$ = immune cells attacking the infected tumour cells.

Proposition 2.3.

The function of tumour growth $u(r,t)$ is part of a system that holds the following equations in the tumour region:

$$\frac{\partial x}{\partial t} + \frac{1}{r^2}\frac{\partial}{\partial r}(r^2 ux) = \lambda x - \beta xv, \quad (6)$$

$$\frac{\partial y}{\partial t} + \frac{1}{r^2}\frac{\partial}{\partial r}(r^2 uy) = \beta xv - \delta y - kzy, \quad (7)$$

$$\frac{\partial n}{\partial t} + \frac{1}{r^2}\frac{\partial}{\partial r}(r^2 un) = \delta y - \mu n, \quad (8)$$

$$\frac{\partial v}{\partial t} + \mathrm{D}\frac{1}{r^2}\frac{\partial}{\partial r}\left(r^2\frac{\partial v}{\partial r}\right) = \beta\delta y - \gamma v - k_0 vz, \quad (9)$$

$$\frac{\partial z}{\partial t} + \frac{1}{r^2}\frac{\partial}{\partial r}(r^2 uz) = syz - \omega z^2. \quad (10)$$

Here,
λ = proliferation rate of tumour cells,
β = infection rate,
δ = infected-cell lysis rate,
μ = removal rate of dead cells,
D = diffusion coefficient of viruses,
b = burst size of infected cells,
γ = clearance rate of viruses,
k = immune killing rate,
k_0= take-up rate of viruses,
s = stimulation rate of infected cells.

In their book, Friedman and Kao solve the system of equations using the method of characteristics in one dimension, which provides the function of tumour size over time by burst size.

The various models proposed display the efforts of mathematicians and biologists to optimise the important field of OVT, which we study in this paper. A general trend among models is the presence of a system of differential equations describing the relationships between cell species and constants. These are used to solve for the function of tumour growth over time.

The four methods we have discussed, namely: Wodarz et al.'s basic model, Novozhilov et al.'s stochastic model, Abu Rqayiq's dynamical system's theory models, and Friedman and Tao's ODE model, are widely varying. A common trend amongst them is the inclusion of interacting cell species uninfected and infected tumour cells in the region of tumour represented by an unknown function. All methods considered the effect of dynamic variables such as infection rate of cells and the burst size of infected cells, which we will take into account in our model. Both Abu Rqayiq and Friedman and Tao also addressed a key problem in the modern OVT field: the immune system's response to a viral infection, which has a negative effect on the treatment by killing the virus and infected tumour cells, preventing the virus from spreading to eradicate the tumour. Research conducted by Wang, Guo, and Smith in 'A mathematical model of oncolytic virotherapy with time delay' studies the impacts of the immune system on the treatment [2], as it is a problem that is hindering the success of OVT. The research made efforts to overcome this challenge by suggesting a treatment involving repeatedly giving the patient immune suppressive drugs. This, however, caused severe oscillations in tumour load, with decreases noticed immediately after the drug was given, followed by a drastic (but progressively less impactful) increase as the drug wore off. Scientists have varying viewpoints on the use of immune suppressive drugs in OVT, as some believe it assists in eradicating the negative impact of the immune system on the treatment, but others believe it leads to an undesirable instability in the patient and should not be given.

We have studied four models for modelling oncolytic virotherapy and have addressed key issues in the field, including the complexity of the interactions, the host's immune response, and the use of immune suppressive drugs. We have used the general trends of research in this field, specifically the incorporation of certain dynamic variables and a larger system of differential equations, to build the base of our model. The papers evaluated display how mathematically modelling virotherapy helps identify the preferrable virus burst sizes to eradicate the tumour in the least amount of time.

Methods and Data

A mathematical model is the best method of simulating this treatment as it can predict tumour load over time. Based on these results, medical practitioners can make decisions to increase the treatment success. Mathematically modelling OVT is less costly than attempting variations of the treatment on patients to determine the optimal treatment. A mathematical model is cheaper and doesn't risk the life and wellbeing of patients upon whom OVT may be tested. The model can be run on a computer many times, and with widely available data online, we can identify the best parameter values to use in the treatment.

This study has developed a machine learning mathematical model to simulate OVT. We have created a deterministic model, inspired by the *Cancer Therapy* chapter in Friedman and Kao's book [8] that analyses the growth of a tumour over time, using data from previous papers to run the simulation. We have implemented a system of ODEs and solved them to plot the function of tumour load over time. This method is a more developed version of the basic system used by Wodarz, where he presents a two-population model including infected and uninfected tumour cells.

The model consists of four populations of cells in the tumour. The first of these are cancer cells uninfected by the virus and the second are tumour cells infected by the virus. Third, the population of dead cancer cells is included, where death is caused by lysis from the virus. Finally, we looked at free viruses in the tumour region, as this has a direct effect on the change in number density of the first three populations, first infecting them, and then killing them.

The population of uninfected cells was initialised to (at timestep 0) $0.84 \cdot 10^6$ cells/mm^3, the population of infected tumour cells to $0.1 \cdot 10^6$ cells /mm^3, and the free virus population to $5 \cdot 10^8 \cdot e^{-1}$ cells/mm^3. These are appropriate initialisation conditions as they represent a small tumour at the beginning of its life, allowing the model to simulate the complete progression of illness. The tumour radius was initialised to 2 mm (diameter = 4 mm), small compared to the average diameter of 47 ± 13 mm [13].

The model uses multiple parameters to define the relationships between populations, presented in the Table 1. The parameters rates of proliferation and infection contribute to the equations for infected and uninfected tumour cells. The rates of lysis and removal of dead cells are involved in plotting the number density of dead cells. The diffusion coefficient, burst size and clearance rate affect the abundance of free viruses in the tumour. In our model, we have primarily used the same parameter values as Friedman and Kao [8].

Table 1. A table showing the parameters in our model

Symbol	Description	Value	Unit
λ	Proliferation rate of tumour cells	2.0	1/h
β	Infection rate	$0.07 \cdot b$	mm^3/h per virus
δ	Infected-cell lysis rate	100/18	1/h
μ	Removal rate of dead cells	100/48	1/h
D	Diffusion coefficient of viruses	3.6	mm^2/h
b	Burst size of infected cells	*various*	virus/cell
γ	Clearance rate of viruses	2.5	1/h
k	Immune killing rate	$2 \cdot 10^{-8}$	mm^3/h per immune cell
k_0	Take-up rate of viruses	10^{-8}	mm^3/h per immune cell
s	Stimulation rate of infected cells	$5.6 \cdot 10^{-7}$	mm^3/h per infected cell

The model was coded with a combination of programming languages Python and MATLAB. We used a freely available software Octave, a high-level programming platform similar to MATLAB to run our model

and produce graphs. Octave is a GNU project software that helps solve numerical problems using MATLAB language and allows for analysis and designing of systems and functions.

The results produced by our paper include an analysis of the burst sizes of different viruses, and which burst sizes lead to the quickest elimination of a tumour. We use statistical methods including multiple hypotheses testing to assess the overall effects of virotherapy treatment on a tumour. We use different initial conditions and parameter values from papers studied, and compare our results, exploring which are values most successful. We also run the Hopf bifurcation of our model to identify stable equilibrium points to better graph the function of tumour size over time.

Model Simulation

At the beginning of the model, the number of timesteps for which the tumour load is calculated is initialised to N = 48 + 1. The greater N is, the more accurate the function plotted, and the longer the code takes to run. For N = 48 + 1, our model took ~40 minutes to run. By contrast, for N = 200 + 1, it took ~ 9.5 hours to produce the graph for 1 burst size, suggesting that the entire simulation would take ~48 hours to run. This demonstrates the extensive increase in run time as timesteps increase.

```
N = 48+1;
dx = 1/(N-1);
xx = (0:(N-1))'*dx;
dt = 0.5*(dx)^2
Tmax = 15*24/100;
```

Other variables are initialised, such as time Tmax to 15*24/100 hours. The tumour is set to boundaries R = 0, and each of the four populations U, X, Y, V are initialised to 0.

```
R = zeros(1,max_iter)
U = zeros(N,1); X = zeros(N,1); Y = zeros(N,1); V = zeros(N,1);
U1 = zeros(N,1); X1 = zeros(N,1); Y1 = zeros(N,1); V1 = zeros(N,1);
U2 = zeros(N,1); X2 = zeros(N,1); Y2 = zeros(N,1); V2 = zeros(N,1);
```

The model plots tumour load over time for five different burst sizes, running through a for loop for each burst size (5, 6, 8, 18 and 27 shown below). In each run, a counter plot_iter increments, and a new line is plotted. The graph's colours for the 5 burst sizes are set to blue, green, cyan, magenta and yellow, using the acronym 'bgrcmy'.

```
plot_iter = 0;
col = 'bgrcmybgrcmy';
```

The parameters beta, delta, gamma etc. are initialised at the start of the loop and used in equations further in the model. We vary the values used for these parameters and analyse the changes in results in order to identify the optimum initialisations.

```
for burst = [5 6 9 18 27];
  plot_iter = plot_iter+1;
  beta = 0.07*burst;
  D = 3.6;
  delta = 100/18;
  gamma = 2.5;
  mu = 100/48;
  theta = 1;
```

The main part of the model consists of code that solves the number densities of the different populations in relation to each other, using the differential equations presented by Friedman and Kao [8]. At each timestep i, we find the values of X1 and Y1 as inductions of X and Y. To do this, we use address the relationships between parameters, rates, and populations similar to those presented in Wodarz's model [4].

```
for i = 1:N
  A = (U(i)-xx(i)*U(N))/R(iter+1);
  F = (lambda*X(i)-mu*(theta-X(i)-Y(i)))/theta;
  if i==1 || i==N
    X1(i) = X(i) + dt*(lambda*X(i)-beta*V(i)*X(i)-F*X(i));
    Y1(i) = Y(i) + dt*(beta*V(i)*X(i)-delta*Y(i)-F*Y(i));
  else
    X1(i) = X(i) - dt*A*(X(i)-X(i-1))/dx+dt*(lambda*X(i)-beta*V(i)*X(i)-F*X(i));
    Y1(i) = Y(i) - dt*A*(Y(i)-Y(i-1))/dx+dt*(beta*V(i)*X(i)-delta*Y(i)-F*Y(i));
  end
```

The changing values of each of the populations, listed in the legend as X, Y, U, and V, are plotted in a graph 'Figure 1', as shown in Figure 5.

```
if mod(iter,20)==0
  figure(1);
  plot(xx,X1,xx,Y1,xx,U1,xx,V1)
  legend('X','Y','U','V')
  title(['T = ' num2str((iter-1)*dt) ' R = ' num2str(R(iter))]);
  drawnow
end
```

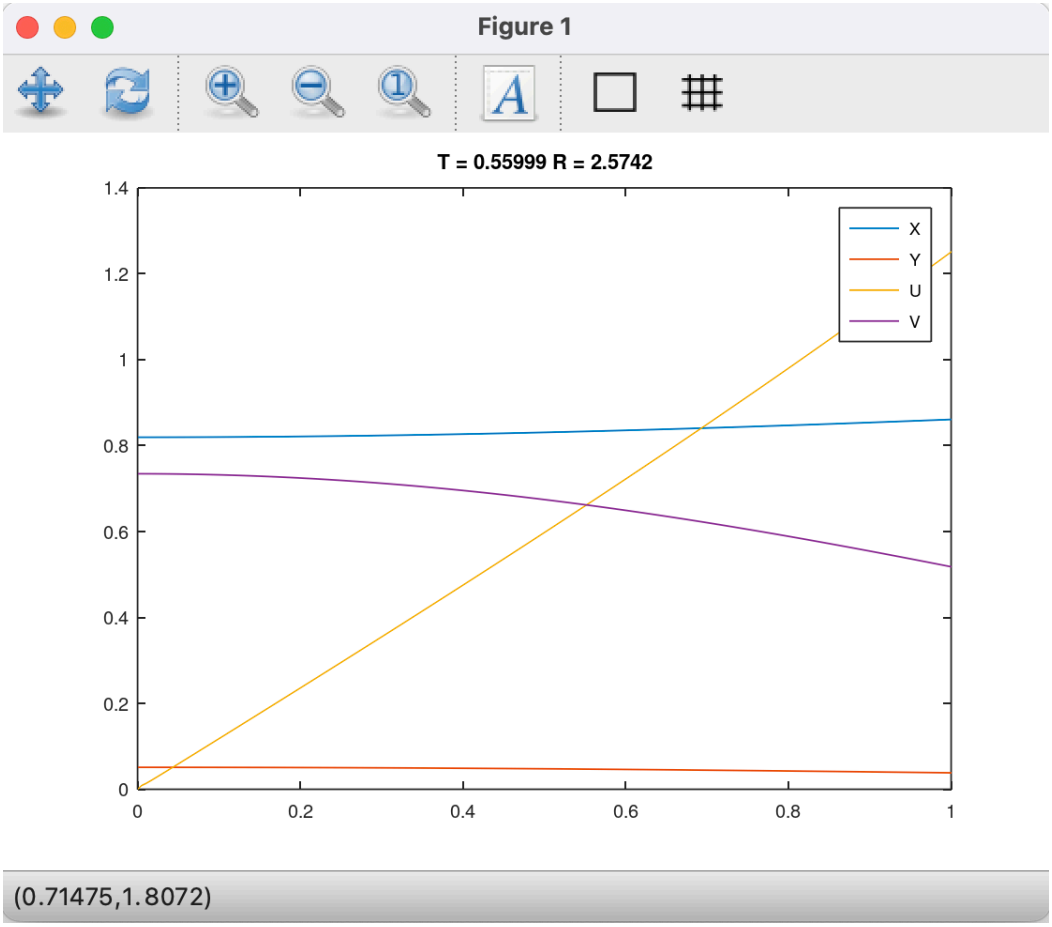

Figure 5. Our model's 'Figure 1' being plotted during a run

The graph updates at each timestep T. They are then combined to plot the graph 'Figure 2', which represents the overall tumour load over time for that particular burst size.

```
figure(2);
hold on;
plot(t*100/24,R,col(plot_iter));
title('R')
save(['burst_' num2str(burst) '.mat'])
```

The variables are then reset, and all calculations repeated for four more burst sizes.

Results and Analysis

First Simulations

For the first simulations and numerical results of our model, we use the same parameters as Friedman and Kao [8], summarised in Table 1. These parameter values are $\lambda = 1$, D = 3.6 and $\gamma = 2.5$. Figure 6 shows our implementation of the burst sizes used in the book '*Mathematical Modeling of Biological Processes*', namely b=25,

50, 100, 150 and 200. This graph shows that the relative tumour load increases dramatically for burst size b=50, from 2 to 10. The graph for this burst size shows a constant tumour load for the first 5 days, before increasing exponentially until the end of the simulation timeframe. It may be possible that the tumour size continues growing, but eventually does peak, however this is an assumption that cannot be confirmed by this graph, as the model has a limit of 15 days.

The treatment's effect of worsening the tumour is reduced with a larger burst size 100, with which the size initially reduces before a negative response triggers an increase. The effectivity is further improved with b=150, for which tumour size decreases constantly for at least 14 days. Surprisingly, burst size b=200 is not plotted on the graph at all. It is possible that this is because the burst size is too large, and thus causing an immediate elimination of *all* tumour cells. This could mean that the graph remains on the x-axis, explaining why it is not visible. However, with the given parameters, the most efficient virus would be one with a burst size of 25. This is because the virus doesn't spread too quickly, triggering the body's immune response, and negating the treatment's effect. The tumour load of such a virus is reduced to near 0 after a time of 15 days.

The second simulation of our model used a smaller range of burst sizes focused on identifying the most effective parameters near the most successful value of the initial simulation, b=25. Figure 7 shows that progressively increasing burst sizes 4, 9, 15 and 25, below a certain threshold, have decreasing tumour loads overall that still individually grow over time. It is not clear why burst size b=25 decreases tumour load in Figure 6 but consistently grows in the second graph. Figure 7 cannot confirm the extrapolation of this trend, as there can be the case where the tumour load peaks and decreases after a certain time, usually due to the numerical density of free viruses overcoming the innate immune response.

Thus, we extended the timeframe of our model, doubling it to 30 days, to show that no burst size less than 50 decreases tumour load. Contrary to our hypothesis, the tumour size increased exponentially for every burst size in Figure 8, not conforming to the case where tumour load peaks before decreasing. It was noticed that the initial tumour loads, in Figure 8 (days 1-15), seem very low in comparison to the later days (15-30); this is because the scale has been enlarged as the tumour load rises dramatically from less than 50 to over 200 in the second set of 15 days. Burst size b=50 was the more effective than the others, changing at a slower rate, however still caused a significant increase in tumour size. It is likely that if the timeframe were to further increase, the load for this burst size would continue growing at a quicker rate.

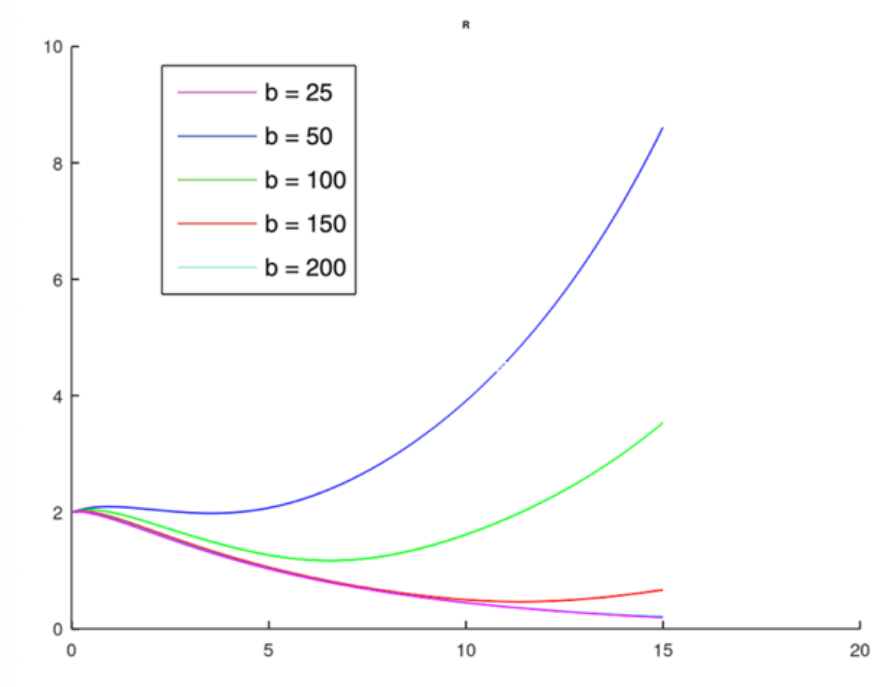

Figure 6. Our model's simulation using burst sizes b=25, 50, 100, 150, 200

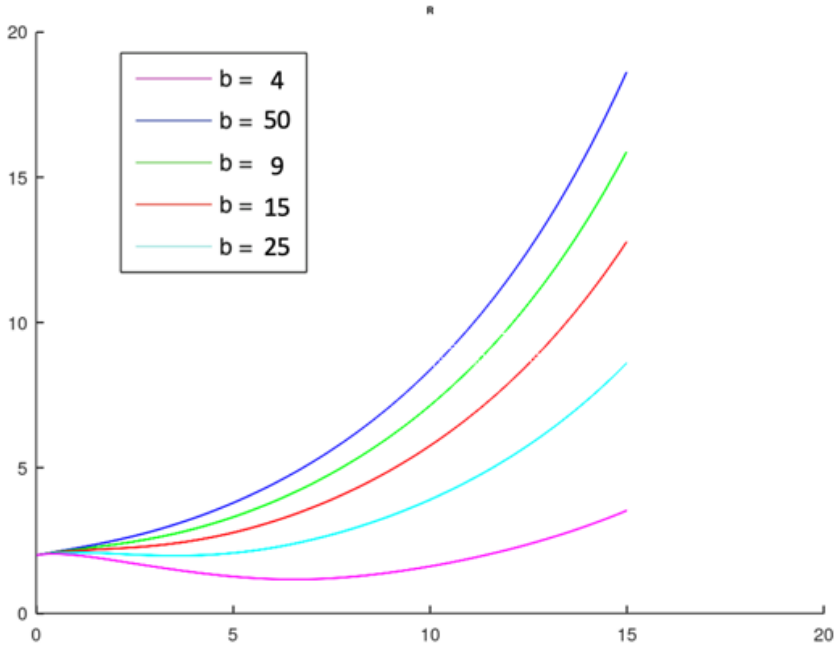

Figure 7. Our model's simulation using burst sizes b=4, 9, 15, 25, 50

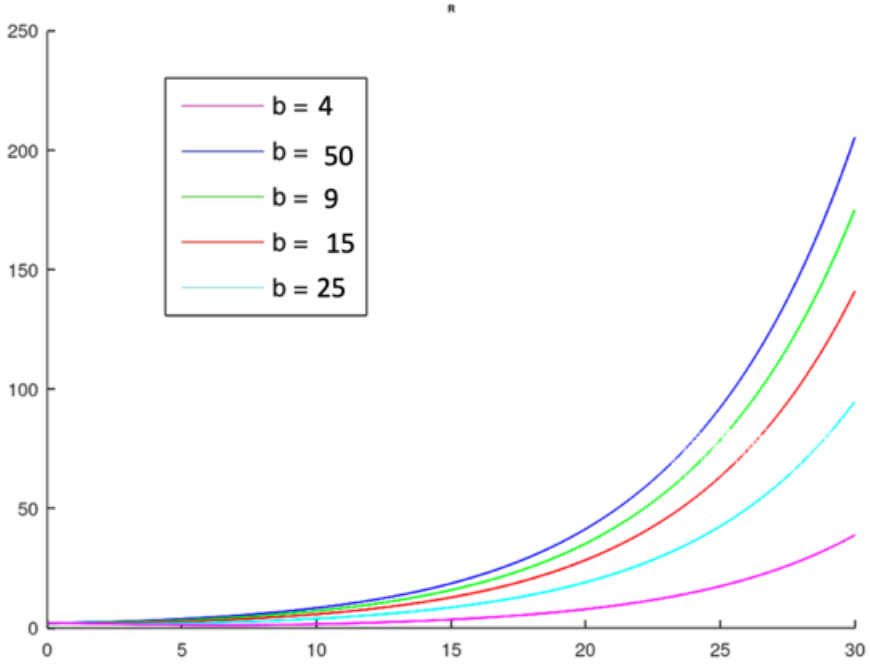

Figure 8. Our model's simulation using burst sizes b=4, 9, 15, 25, 50 with an extended timeframe of 30 days

Second Simulations

We also simulated our model using the parameters from *'Mathematical Modeling and Dynamics of Oncolytic Virotherapy'* [1]. His paper stated that the basic model gives stable equilibrium points between the thresholds $5<b<27.766$, with b representing the burst size of the virus. We attempted to graph the tumour loads of several burst sizes between these thresholds to confirm the presence of stable points, where the tumour size decreases over time. In this simulation, we maintained the initial boundary conditions and parameters from our previous runs (Figures 6-8). Figure 9 presents the tumour load over time for burst sizes b=5,6,9,18 and 27, covering a range of sizes between both critical values.

Figure 9 shows that every burst size leads to an increased tumour load after 15 days, not conforming to Abu-Rqayiq's thresholds. In contrast to Figure 6, where smaller burst sizes were more efficient at reducing tumour load (such as b=25 being better than 100 and 150), in Figure 9, the opposite is observed. The graph shows that smaller burst sizes 5, 6 and 9 caused the quickest tumour growth, with a relative size increase from 2 to 20 in just 15 days. On the other hand, burst sizes 18 and 27 were progressively more efficient, confirming our hypothesis that burst sizes around 25 are optimal (as depicted in Figure 6).

In hopes of finding that tumour load peaked after a greater time and eventually decreased, we ran our simulations using Abu-Rqayiq's thresholds for larger timeframes: 30 and 100 days. In the case that this occurred, our graphs would mimic Novozhilov et al.'s initial results, where an increase in tumour load was found before its elimination. This is shown in graph (a) in Figure 3. However, the results for both timeframes 30 and 100 days, presented in Figures 10 (30 days) and 11 (100 days), show an exponential increase in tumour load, as opposed to the desired decrease. Figure 10 shows a dramatic increase in all burst sizes, with the load for b=5 as 200 after 30 days. This trend of increasing continued from days 30-100 in Figure 11. Here, all burst sizes ended with a tumour load of between 5,000,000 and 15,000,000, clearly showing that Abu-Rqayiq's thresholds were not compatible with our model's equations.

Another change in method we attempted to produce successful results using Abu-Rqayiq's dataset was to change the number of timesteps N. In addition to the original number N = 48 + 1, we ran our model with N = 200 + 1 (with an extended timeframe of 30 days). Figure 12 shows that a larger number of timesteps N = 201 increases the accuracy of the graph, but very little changes visibly, despite taking 9.5 hours to be produced. We produced the graph for only burst size b=5 given the extensive time required for the model to be simulated with 201 timesteps. In Figure 12, the graph is almost identical to that in Figure 10. It is very similar to the graph in Figure 10 as well, with the difference being that the graph continually extends until 30 days.

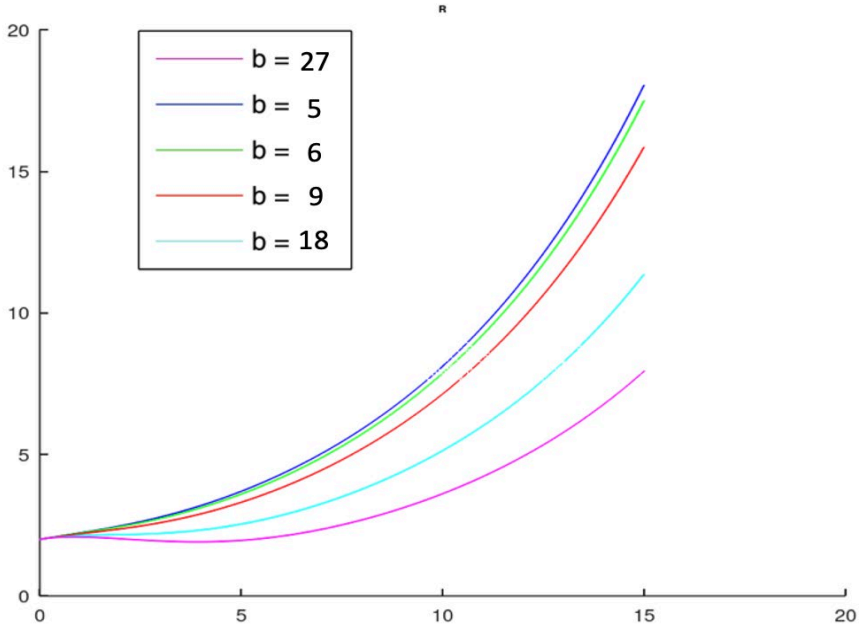

Figure 9. Our model's simulation using burst sizes b=5, 6, 9, 18, 27

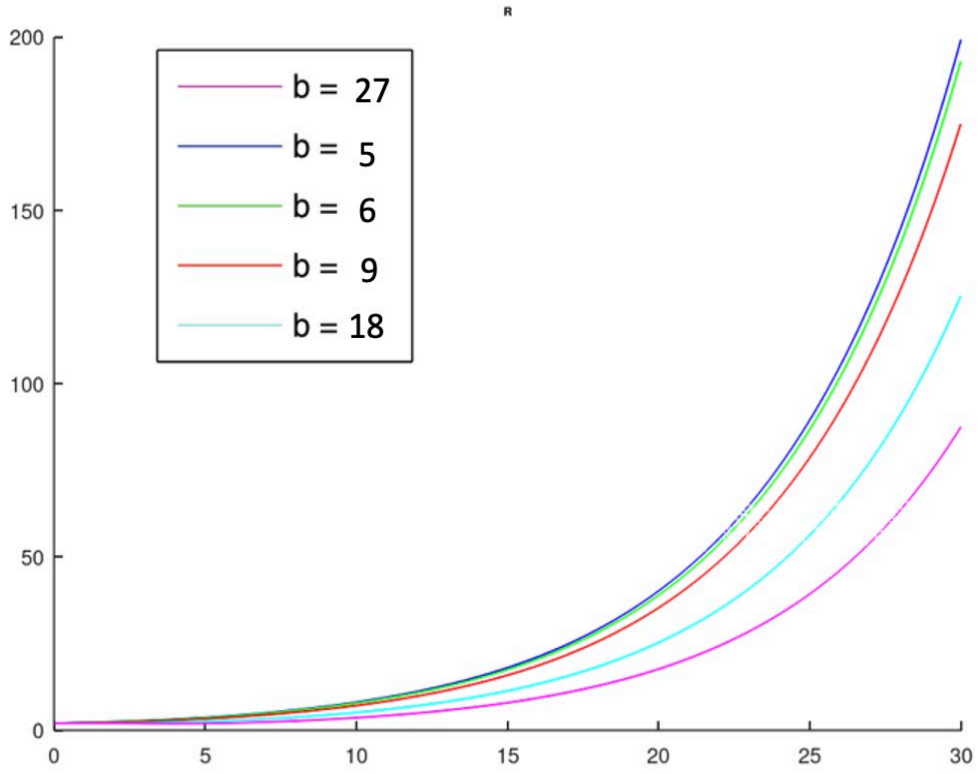

Figure 10. Our model's simulation using burst sizes b=25, 50, 100, 150, 200 with an extended timeframe of 30 days

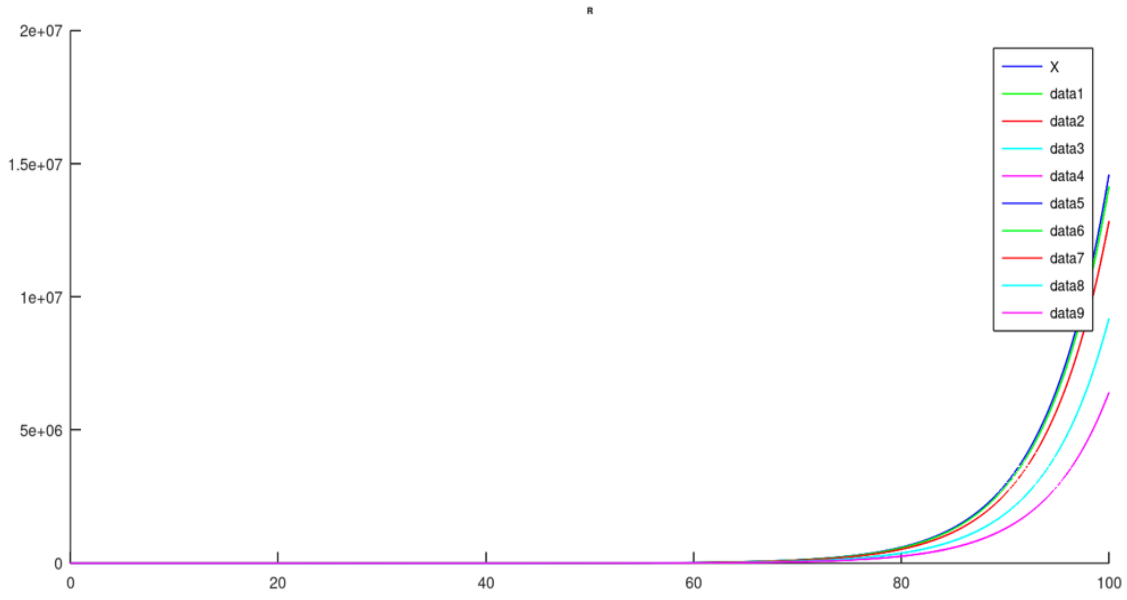

Figure 11. Our model's simulation using burst sizes b=25, 50, 100, 150, 200 with an extended timeframe of 100 days

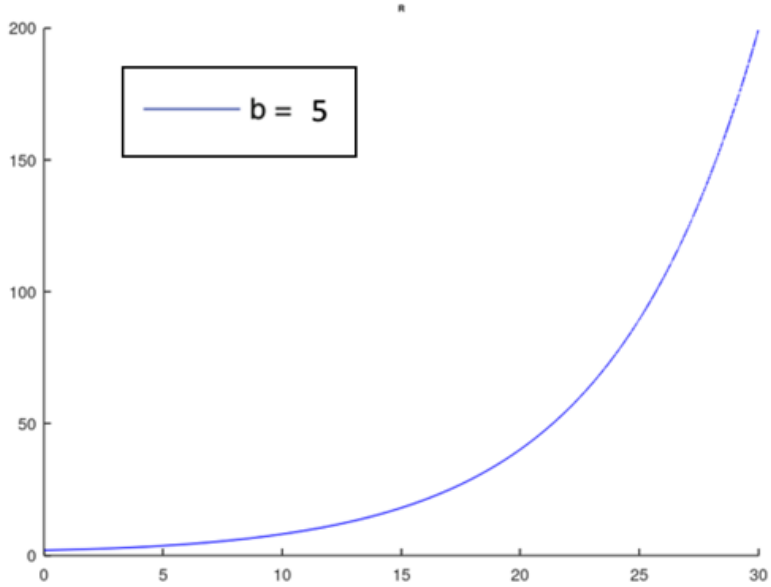

Figure 12. Our model's simulation using burst sizes b=25, 50, 100, 150, 200 with an increases number of timesteps

Hopf Bifurcation

Bifurcation is a theory that focuses on how a system, dependent on a certain parameter, changes with that parameter p. The system would have various bifurcation points where the system's behaviour changes radically as a parameter p passes a critical value p_{cr}. In the case of cells in a tumour, we will run bifurcation on different parameters and observe how the populations in the tumour change to identify parameter thresholds.

Some systems can present oscillations around certain thresholds. Such a system has a stable equilibrium – a lack of change in behaviour – if the parameter p crosses a critical value p_{cr} leading to a series of periodic solutions; this is called Hopf bifurcation. The bifurcation can be represented by differential equations and then solved using the Euler method.

We have used MATLAB to program an algorithm that plots the bifurcation of differential equations. Our model has 4 differential equations; however, it is not possible to plot their bifurcations on one graph, which would require it to be 4-dimensional. Thus, we have plotted the bifurcations of combinations of pairs of the 4 differential equations on 2-dimensional graphs.

Equation (11) shows the first two differential equations for the bifurcation of populations of uninfected and infected tumour cells. We simplified the equations by replacing variables with constants such that only one parameter β (infection rate) remained. Here, the ODEs are

$$\frac{dx}{dt} = 2x - 10\beta x, \quad \textit{and} \quad \frac{dy}{dt} = 10\beta x - \frac{100}{18}y. \tag{11}$$

Similarly, equation (12) shows the behaviour of a system of populations of dead cells and free virus particles in the tumour dependent on the variable δ (infected cell lysis rate). Here,

$$\frac{dn}{dt} = \delta y - \frac{100}{48}n, \quad and \quad \frac{dv}{dt} = 0.07\delta y - 2.5v. \tag{12}$$

The bifurcation for these pairs of equations was run on a specific Hopf model we developed.

Optimal Viruses

Based on the results produced from our model, we found that the best burst size for a virus used in OVT is b=25. Our simulations that ran using Abu-Rqayiq's thresholds of 5< b<27.766 confirmed this, as the graph for burst size 25 displayed a tumour remission in Figure 6. Our research on oncological viral drugs that have a replication burst size of around 25 has produced three optimal viruses.

Firstly, the alpha virus used in Max Delbrück's study had optimal burst sizes [10]. Of the 150 samples which showed bursts, 4 were less than 25, while 21% were below 100. The burst sizes ranged from 20 to over 1000, with most below 200. The features of this virus are optimum to match our model's results.

Secondly, a modified herpes simplex virus (HSV) can be used. Koelle and Wald's study into the pathogenesis of this virus [11] has found that this virus replicates with a relatively low burst size of between 100-1000 daughter virions per infected cell. Wang's study into modelling OVT has also found that HSV-1 has a potential use in the treatment [2].

Thirdly, the adenovirus ONYX-015, modified to specifically activate p53 – a tumour suppressor protein – in infected tumour cells with an altered p53 pathway, is a viable treatment. This has already had success in clinical trials and tests. Ries and Korn's study into the efficacy of ONYX-015 for human tumours evaluated that three of 22 patients (14%) experienced tumour responses, ten patients (45%) showed stabilisation of their disease, and all but one patient developed increased antibody levels after treatment [14]. These promising results suggest that the ONYX-015 virus is an advanced and successful replication-competent virus for cancer therapy.

Discussions and Limitations

A major limitation of our research was the success the model; the finding of an efficient cancer treatment was heavily dependent on the results that the model produced. If, despite various attempted parameters and burst sizes, all graphs still displayed and increase in tumour size, then there would be no efficient treatment found by this model.

The model's simulation, being a heavy program, took a very long time to run. With 49 timesteps, the model ran for about 40 minutes, however, with 201 timesteps, it took 9.5 hours to produce just $\frac{1}{5}$ of the graph. This meant that producing results was incredibly time consuming: a problem that could not be solved without a more powerful computer. Our model includes several separate functions and for-loops, minimizing the number of lines and run-time. However, the negative impact of this roadblock could be reduced further by implementing more abstraction in the code. This would simplify the code and ensure that it runs smoothly. Another solution would be to utilise parallelisation to reduce computational time, allowing the model to run quicker overall.

Another limitation was the lack of existing data regarding cancer tumours treated with OVT. This made it difficult to compare our results with others', as there were only a couple of papers studying the effects of this new treatment on cancerous tumours. We initially were concerned that data found would be too large and thus difficult to process. This meant sourced data would require a lot of effort to clean (to remove noise effects like unnecessary data or anomalies). As we did not find enough data to support our results, this was not an issue in this paper. However, if data is sourced from online published articles or hospitals that perform OVT, this may become a serious roadblock.

Summary and Future Work

In this paper, we have studied OVT and have reviewed previous studies that have modelled the treatment. These include: Wodarz's basic model for killing p53-negative cancer which proposed the basic model and assessed the ideal conditions for replicating and nonreplicating viruses [4], Novozhilov's mathematical modelling of tumour therapy which proposed a deterministic model developing Wodarz's model [7], Abu-Rqayiq's studies of multiple types of models including a model with an immune response, and a fractional derivative approach [1], and Friedman and Kao's chapter on treating cancer using viruses [8].

From the conclusions of the four papers studied, we developed a mathematical model to simulate the changing populations of cells in a tumour over time. We used conditions from previous papers, and produced results after varying parameters, timeframes, and the burst size of the virus. We also implemented Hopf bifurcation in our model.

In the future, we could utilise parallel computing. This is the process of breaking down a heavy program into smaller parts that can be run simultaneously on separate processors communicating via a shared memory. Parallelisation would result in multiple CPUs processing the simulation of our model, which reduce the time needed to run it and produce results.

We could attempt a more detailed analysis of the stable equilibrium points of our models by developing a more advanced Hopf bifurcation program that produced results studying different types of bifurcation, such as supercritical, saddle-point, pitchfork, and steady-state bifurcation. This would help to understand the behaviours of populations better as parameters changed.

Supplements

We have presented the MATLAB code and related documents for our OVT and bifurcation models on the following Github site, accessible at: https://github.com/ajobapa/OVTModel.

Tables and Figures

Table 1 shows the parameters in our model.
Figure 1 shows a summary and relations of different mathematical models and papers representing OV cancer treatment.
Figure 2 shows the different domains which produce different system equilibria.
Figure 3 shows the results of Novozhilov's model simulation.
Figure 4 shows Abu-Rqayiq's model parameters.
Figure 5 shows our model's 'Figure 1' being plotted during a run.
Figure 6 shows model's simulation using burst sizes b=25, 50, 100, 150, 200.
Figure 7 shows our model's simulation using burst sizes b=4, 9, 15, 25, 50.
Figure 8 shows our model's simulation using burst sizes b=4, 9, 15, 25, 50 with an extended timeframe of 30 days.
Figure 9 shows our model's simulation using burst sizes b=5, 6, 9, 18, 27.
Figure 10 shows our model's simulation using burst sizes b=5, 6, 9, 18, 27 with an extended timeframe of 30 days.
Figure 11 shows our model's simulation using burst sizes b=5, 6, 9, 18, 27 with an extended timeframe of 100 days.
Figure 12 shows our model's simulation using burst sizes b=5, 6, 9, 18, 27 with an increased number of timesteps.

Acknowledgments

I would like to thank my advisor for the valuable insight provided to me on this topic.

References

[1] Abu-Rqayiq, A. (2021, April 23). Mathematical Modeling and Dynamics of Oncolytic Virotherapy. Retrieved from https://www.intechopen.com/chapters/76116. doi: 10.5772/intechopen.96963

[2] Wang, Z., Guo, S., & Smith, H. (2019, March 6). A mathematical model of oncolytic virotherapy with time delay[J]. Mathematical Biosciences and Engineering, 2019, 16(4): 1836-1860. Retrieved from https://www.aimspress.com/article/id/3453. doi: 10.3934/mbe.2019089

[3] Cancer Survival Statistics (2023, September 27). Cancer Research UK. Retrieved from https://www.cancerresearchuk.org/health-professional/cancer-statistics/survival#:~:text=Many%20of%20the%20most%20commonly,more%20(2010%2D11)

[4] Wodarz, D. (2003, January 20). Gene Therapy for Killing p53-Negative Cancer Cells: Use of Replicating Versus Nonreplicating Agents. Human Gene Therapy, 2003, 14(2): 153-159. Retrieved from https://www.liebertpub.com/doi/10.1089/104303403321070847. doi: 10.1089/104303403321070847

[5] Norman, K.L, Farassati, F., & Lee, P.W. (2001, June-September). Oncolytic viruses and cancer therapy. Retrieved from https://pubmed.ncbi.nlm.nih.gov/11325607/

[6] Wein, L.M., Wu, J.T., & Kirn, D.H. (2003, March 15). Validation and analysis of a mathematical model of a replication-competent oncolytic virus for cancer treatment: implications for virus design and delivery. Retrieved from https://pubmed.ncbi.nlm.nih.gov/12649193/

[7] Novozhilov, A.S., Berezovskaya, F.S., Koonin, E.V., & Karev, G.P. (2006, February 17). Mathematical modeling of tumor therapy with oncolytic viruses: Regimes with complete tumor elimination within the framework of deterministic models. Retrieved from https://www.ncbi.nlm.nih.gov/pmc/articles/PMC1403749/. doi: 10.1186/1745-6150-1-6

[8] Friedman, A., & Kao, C-Y. (2014). Mathematical Modeling of Biological Processes. Springer International Publishing Switzerland.

[9] Friedman, A., & Tao, Y (2003, November). Analysis of a Model of a Virus that Replicates Selectively in Tumor Cells. Journal of Mathematical Biology. Retrieved from https://pubmed.ncbi.nlm.nih.gov/14605856/

[10] Delbrück, M. (1945). The Burst Size Distribution in the Growth of Bacterial Viruses (Bacteriophages). Retrieved from https://journals.asm.org/doi/pdf/10.1128/jb.50.2.131-135.1945

[11] Koelle, D.M., & Wald, A. (2000). Herpes simplex virus: the importance of asymptomatic shedding. Journal of Antimicrobial Chemotherapy, 2000, 45: Topic T3, 1-8. Retrieved from https://watermark.silverchair.com/

[12] Tian, J.P. (2011). The replicability of oncolytic virus: defining conditions in tumor virotherapy. Retrieved from https://pubmed.ncbi.nlm.nih.gov/21675814/

[13] J Bone Oncol, 2019, 14. Retrieved from https://www.ncbi.nlm.nih.gov/pmc/articles/PMC6348933/. doi: 10.1016/j.jbo.2018.100211

[14] Ries, S., & Korn, W.M (2002). ONYX-015: Mechanisms of action and clinical potential of a replication-selective adenovirus. British Journal of Cancer, 86: 5-11. Retrieved from https://www.researchgate.net/publication/11504842_ONYX-015_Mechanisms_of_action_and_clinical_potential_of_a_replication-selective_adenovirus
Equilibrium Solutions (n.d.). Study Pug. Retrieved from https://www.studypug.com/differential-equations-help/equilibrium-solutions#:~:text=If%20nearby%20solutions%20to%20the,have%20an%20unstable%20equilibrium%20point
Heijden, G. (n.d.). Hopf Bifurcation – UCL. Retrieved from https://www.ucl.ac.uk/~ucesgvd/hopf.pdf

Jacobian Matrix and Determinant (Definition and Formula) (2019, December 9). BYJUS. Retrieved from https://byjus.com/maths/jacobian/

Law of Mass Action – Definition, Application & Equation with Statement (2022, August 19). BYJUS. Retrieved from https://byjus.com/chemistry/law-of-mass-action-or-law-of-chemical-equilibrium/

Khan, F.A., Akhtar, S.S., & Sheikh, M.K. (2005, January). Cancer Treatment – Objectives and Quality of Life Issues[J]. Malays J Med Sci, 2005, 12(1): 3-5. Retrieved from https://www.ncbi.nlm.nih.gov/pmc/articles/PMC3349406/

Kumar, P., Erturk, V.S., Yusuf, A., & Kumar, S. (2021, June 19). Fractional time-delay mathematical modeling of Oncolytic Virotherapy[J]. Chaos, Solitons & Fractals, 2021, 150. Retrieved from https://www.sciencedirect.com/science/article/abs/pii/S096007792100477X. doi: 10.1016/j.chaos.2021.111123

What is Cancer (n.d.). National Cancer Institute. Retrieved from https://www.cancer.gov/about-cancer/understanding/what-is-cancer#:~:text=Cancer%20is%20a%20disease%20in,up%20of%20trillions%20of%20cells

What is Parallel Computing? Definition and FAQs (n.d.). HEAVY.AI. Retrieved from https://www.heavy.ai/technical-glossary/parallel-computing#:~:text=Parallel%20computing%20refers%20to%20the,part%20of%20an%20overall%20algorithm

Zou, C. et al. (2018, December 14). Managements of giant cell tumor within the distal radius: A retrospective study of 58 cases from a single center.